THE ASTROPHYSICAL JOURNAL, 435:L35–L38, 1994 November 1

HST FOS SPECTROSCOPY OF M87: EVIDENCE FOR A DISK OF IONIZED GAS AROUND A MASSIVE BLACK HOLE[1]

RICHARD J. HARMS,[2] HOLLAND C. FORD,[3,4] ZLATAN I. TSVETANOV,[3] GEORGE F. HARTIG,[4] LINDA L. DRESSEL,[2] GERARD A. KRISS,[3] RALPH BOHLIN,[4] ARTHUR F. DAVIDSEN,[3] BRUCE MARGON,[5] AND AJAY K. KOCHHAR[2]

Received 1994 May 19; accepted 1994 August 15

ABSTRACT

Using the Faint Object Spectrograph on the *Hubble Space Telescope* (*HST*) to observe the central region of M87, we have obtained spectra covering ~4600–6800 Å at a spectral dispersion ~4.4 Å per resolution element through the 0".26 diameter entrance aperture. One spectrum was obtained centered on the nucleus of M87 and two centered 0".25 off the nucleus at position angles of 21° and 201°, thus sampling the anticipated major axis of the disklike structure (described in a companion *Letter*) expected to lie approximately perpendicular to the axis of the M87 jet. Pointing errors for these observations are estimated to be less than 0".02. Radial velocities of the ionized gas in the two positions 0".25 on either side of the nucleus are measured to be $\approx \pm 500$ km s^{-1} relative to the M87 systemic velocity. These observations plus emission-line spectra obtained at two additional locations near the nucleus show the ionized gas to be in Keplerian rotation about a mass $M = (2.4 \pm 0.7) \times 10^9\ M_\odot$ within the inner 0".25 of M87. Our results provide strong evidence for the presence of a supermassive nuclear black hole in M87.

Subject headings: black hole physics — galaxies: individual (M87) — galaxies: kinematics and dynamics — instrumentation: spectrographs

1. INTRODUCTION

While circumstantial evidence for black holes as the ultimate power source in active galactic nuclei (AGNs) is ubiquitous, convincing observations are in short supply. Any evidence for black holes is necessarily indirect. Our best evidence for stellar black holes is from the dynamical analysis of galactic X-ray binaries. The dynamics of millions of stars plus gas in galactic nuclei is necessarily more complex, but black holes can imprint their signature on both the morphology and the kinematics of stars and gas in the centers of galaxies. As with stellar-mass black holes, the most convincing case is dynamical evidence for mass-to-light ratios incompatible with astrophysical manifestations of ordinary matter.

As the host of the powerful radio source Virgo A, the nearby giant elliptical galaxy M87 has been a favorite target in the search for massive black holes. A central black hole would provide a plausible source for the energy to power the relativistic jet in M87, and its proximity provides a good scale for seeing the interaction of the black hole with the surrounding galaxy. A sharp rise in the velocity dispersion profile of M87 led Sargent et al. (1978) to conclude that the nucleus of M87 harbored a black hole of more than $10^9\ M_\odot$. The interpretation of spectroscopic measurements of M87 from ground-based telescopes, however, has long been ambiguous (Dressler & Richstone 1990) due to the limited angular resolution attainable when observing through atmospheric turbulence. The best subarcsecond resolution spectra of M87 from the ground have been obtained by van der Marel (1994) using the 4.2 m William Herschel Telescope. That there might also be some hope of detecting a central black hole by spectroscopy of emission lines from ionized gas in the nuclear region of M87 was indicated by the results of Ford & Butcher (1979), who detected the presence of at least two distinct velocity systems for ionized gas in the central region of M87.

Studying the variation of surface brightness with position in M87 is a complementary approach for detecting the possible presence of a central black hole. The centrally peaked distribution of the stellar light in the nucleus of M87 has been interpreted by Young et al. (1978) as evidence for a central black hole of mass $M_{BH} \approx 2.6 \times 10^9\ M_\odot$. Similarly, by deconvolving (spherically aberrated) images taken with the WF/PC1, Lauer et al. (1992) show that the surface brightness profile is consistent with a central black hole of mass $M_{BH} \geq 10^9\ M_\odot$, but that velocity measurements within the central 0".5 would be needed to establish this conclusively.

As described in a companion *Letter* (Ford et al. 1994), the high-resolution Wide Field/Planetary Camera-2 (WFPC2) images of the central regions of M87 show an apparent disk-like structure of ionized gas around the galaxy nucleus, oriented approximately perpendicular to the optical jet. This suggests that Nature may have been kind, as measuring emission-line velocities and interpreting the dynamics of a rotating disk are far easier than deconvolving absorption profiles to obtain velocity dispersions and building dynamical models of stellar orbits. Emission lines seen in the two spectra nearest the nucleus clearly show the presence of substantial rotational motion, with the velocities of the two regions differing by ~1000 km s^{-1}.

2. SPECTROSCOPIC OBSERVATIONS

Following the first servicing mission in 1993 December to achieve the originally planned high angular resolution imaging performance of the *HST*, several early release observations (EROs) were conducted to verify the scientific performance of the instruments. To test the high angular resolution performance of the Corrective Optics Space Telescope Axial

[1] Based on observations with the NASA/ESA Hubble Space Telescope obtained at the Space Telescope Science Institute, which is operated by AURA, Inc., under NASA Contract NAS 5-26555.

[2] Applied Research Corporation, Landover, MD 20785.
[3] Johns Hopkins University, Baltimore, MD 21218.
[4] Space Telescope Science Institute, Baltimore, MD 21218.
[5] University of Washington, Seattle, WA 98195.

Replacement instrument (COSTAR) + Faint Object Spectrograph (FOS), we obtained spectra at six positions on and near the nucleus of M87. The first FOS ERO attempt, on 1994 February 11, indicated that the optical performance of the restored *HST* and FOS was excellent, but failed to obtain the desired data due to a pointing error in the Fine Guidance Sensor (FGS) system. The rescheduled observations, obtained on 1994 May 5, were completely successful.

In Figure 1*a* (Plate L20), the six locations for which we obtained spectra are mapped onto the continuum-subtracted Hα + [N II] WFPC2 image of the nuclear region of M87. Circles properly scaled to represent the 0".26 diameter FOS aperture are superposed onto the image. Spectra at positions 1–3 were obtained on 1994 February 11 and those at positions 4–6 on 1994 May 5. The G570H grating used for all these observations covers ~4600–6800 Å. Spectra are quarter-stepped, so that each spectrum consists of slightly over 2000 data points sampled on 1.1 Å intervals. The true spectral resolution using the G570H grating with the 0".26 diameter aperture is 4.15 Å. Exposure times for positions 1–6 were 1000, 4000, 6000, 1000, 3000, and 3000 s, respectively.

The spectra were reduced using the standard *HST* pipeline reduction software. A common wavelength scale was established based on several wavelength calibration spectra taken throughout the observations. Because the post-COSTAR FOS photometric calibration has been completed only for pointlike sources, the pipeline flux values were multiplied by 0.80 based on our estimate of the relative throughput of the FOS 0".26 diameter entrance aperture for extended versus point sources. Our conclusions do not depend on absolute flux values.

The spectra, plotted in Figure 2 (Plate L21), show that the major emission and absorption features vary significantly among the six locations in the nucleus of M87. The spectrum at position 3, just over 2" from the nucleus, shows the typical late-type spectrum of ellipticals, with (broadened) absorption features seen in Na D (λ5893) and Mg *b* (λ5175). Hα appears weakly in emission at this location. Closer to the nucleus, where the Na D and Mg *b* absorption features appear to weaken and broaden, several emission lines dominate the spectra. Emission lines of Hα and Hβ, [O III] ($\lambda\lambda$4959, 5007), [O I] (λ6300), [N II] ($\lambda\lambda$6548, 6584), and [S II] ($\lambda\lambda$6716, 6731) are prominent in the spectra of the five positions lying within ~0".5 of the nucleus.

3. RESULTS

The most dramatic feature of the spectra is evident in Figure 1*b*, which overplots portions of the spectra taken along a direction perpendicular to the jet of M87. As discussed below and in our companion *Letter* (Ford et al. 1994), the major axis of the disk lies approximately perpendicular to the jet. The on-nucleus spectrum (position 4) shows highly broadened emission features, while the spectra for positions 5 and 6, centered 0".25 to either side of the nucleus, are clearly seen to be redshifted and blueshifted by approximately equal amounts. The radial velocity difference between positions 5 and 6 is substantial, $\approx 1000 \pm 100$ km s^{-1} for various emission lines, implying rapid rotation of the disk.

The stronger emission-line features have been analyzed to determine line strengths, heliocentric radial velocities, and instrument-corrected full widths at half-maximum (FWHM), for each of the five regions nearest the nucleus. Table 1 summarizes these results. Several trends are immediately obvious: the emission features become stronger nearer the nucleus, the relative line intensities show little systematic variation with distance from the nucleus, substantial opposite-sign radial velocity shifts are apparent for locations 5 and 6, and the magnitude of these velocity shifts is larger for the high-ionization [O III] than for the lower ionization [S II] and Hβ. The results for Hα are consistent with those for Hβ, but suffer greater uncertainty due to blending with [N II]. The behavior of [O I] follows that of the other low-ionization species, but with greater uncertainty due to its lower signal-to-noise ratio in all the spectra.

The highly broadened emission-line profiles seen on the nucleus (position 4) yield a fairly coarse determination for the systemic velocity. A better determination can be made from the

TABLE 1

M87 EMISSION-LINE PROPERTIES

Location Number	Ion	Line Surface Brightness (10^{-6} ergs cm^{-2} s^{-1} arcsec^{-2})	Mean LOS Velocity (km s^{-1})	FWHM (LOS Velocity) (km s^{-1})
1.....	[O III] $\lambda\lambda$4959, 5007	223 ± 24	1103 ± 21	482 ± 43
1.....	[S II] $\lambda\lambda$6716, 6731	482 ± 59	1139 ± 26	442 ± 45
1.....	[O I] λ6300	92 ± 29	1211 ± 100	703 ± 273
1.....	Hβ λ4861	63 ± 11	1187 ± 47	560 ± 69
2.....	[O III] $\lambda\lambda$4959, 5007	77 ± 12	1100 ± 29	503 ± 83[a]
2.....	[S II] $\lambda\lambda$6716, 6731	176 ± 23	1090 ± 26	419 ± 45
2.....	[O I] λ6300	44 ± 14	1141 ± 83	803 ± 280
2.....	Hβ λ4861	24 ± 5	1115 ± 40	358 ± 91
4.....	[O III] $\lambda\lambda$4959, 5007	1293 ± 164	1160 ± 63	1638 ± 143
4.....	[S II] $\lambda\lambda$6716, 6731	2670 ± 332	1247 ± 216	1822 ± 455
4.....	[O I] λ6300	1534 ± 211	1382 ± 70	1870 ± 187
4.....	Hβ λ4861	470 ± 77	1312 ± 96	1412 ± 232
5.....	[O III] $\lambda\lambda$4959, 5007	303 ± 20	1856 ± 15	636 ± 34
5.....	[S II] $\lambda\lambda$6716, 6731	746 ± 51	1742 ± 21	589 ± 36
5.....	[O I] λ6300	228 ± 15	1770 ± 18	569 ± 43
5.....	Hβ λ4861	127 ± 9	1768 ± 19	528 ± 42
6.....	[O III] $\lambda\lambda$4959, 5007	381 ± 21	739 ± 13	667 ± 33
6.....	[S II] $\lambda\lambda$6716, 6731	695 ± 78	858 ± 37	757 ± 100
6.....	[O I] λ6300	179 ± 21	860 ± 38	808 ± 115
6.....	Hβ λ4861	133 ± 11	857 ± 28	830 ± 72

[a] A single Gaussian provides a poor fit for either of the lines λ4959 or λ5007, each of which appears to contain both a broad and narrow component.

PLATE L20

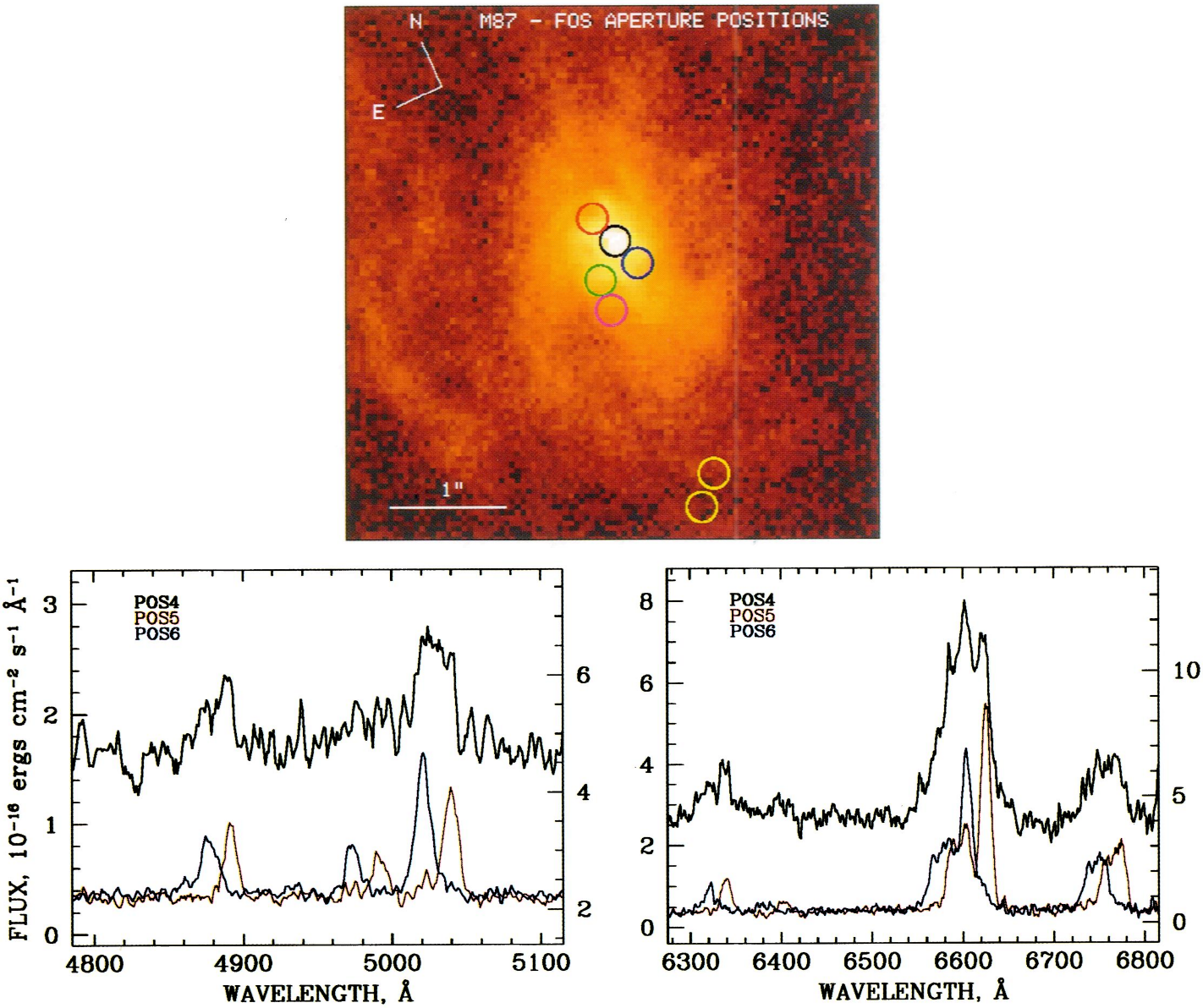

FIG. 1.—(*a*) Continuum-subtracted Hα + [N II] WFPC2 image of the center of M87. Colored circles are drawn to scale to indicate the locations of the FOS spectra. (*b*) Expanded view of two portions of the spectra (smoothed with a three-point boxcar filter to approximate the true resolution for the FOS diode width) taken at the three locations lying along a line perpendicular to the M87 jet. Left-side axes apply to the position 5 and 6 fluxes, right-side axes to the position 4 fluxes. The substantial emission-line velocity shifts between positions 5 and 6, and the highly broadened lines in the on-nucleus (position 4) spectrum, are both readily apparent. The absorption feature observed at position 4 near 4825 Å appears to be real but has not been convincingly identified.

HARMS et al. (see 435, L36)

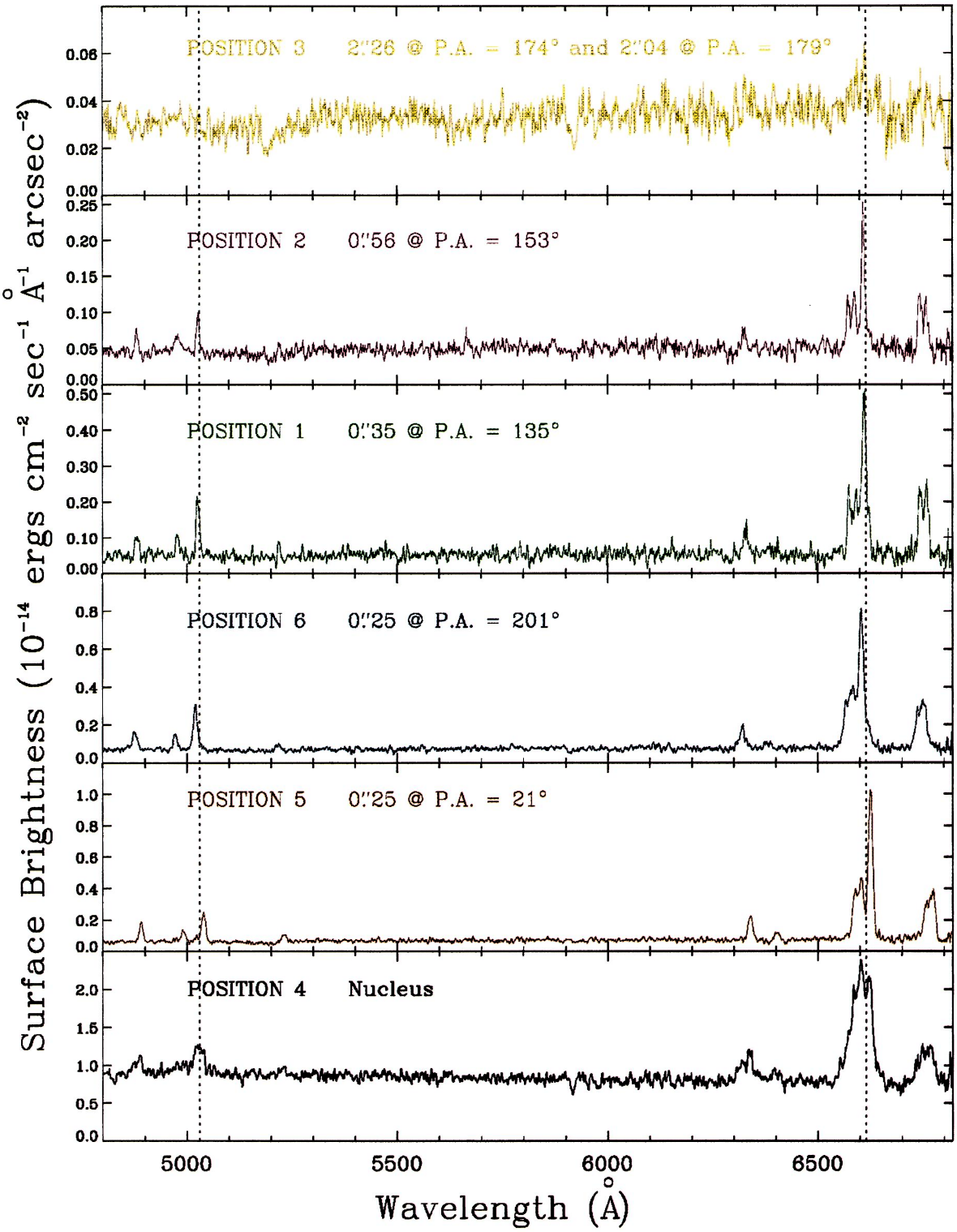

FIG. 2.—FOS spectra at the six locations observed in M87, color-coded to match the corresponding regions shown in Fig. 1*a* and smoothed as in Fig. 1*b*. Superposed dotted lines indicate wavelengths of [O III] λ5007 and [N II] λ6584 at the systemic velocity of M87. Progressing toward the nucleus, the absorption features become less prominent and emission lines become stronger. Velocity shifts of the emission features at positions 1, 2, 5, and 6 imply nearly Keplerian rotation of the disk seen in Fig. 1*a*. Broadened emission lines at position 4 on the nucleus suggest continuing Keplerian rise in velocities interior to positions 5 and 6.

HARMS et al. (see 435, L36)

spectra of the symmetrically located positions 5 and 6, producing an estimated (heliocentric) $V_{sys} = 1309 \pm 12$ km s^{-1} (statistical errors only). These values are slightly higher than the value $V_{sys} = 1277$ km s^{-1} with uncertain systematic errors adopted by van der Marel (1994), but the difference is probably not significantly larger than probable systematic errors in the two measurements. We find, perhaps fortuitously, the same ≈ 40 km s^{-1} smaller velocity for the nucleus than for the immediately surrounding regions as has been noted by Dressler & Richstone (1990) and by van der Marel (1994).

The strongest stellar absorption features in our spectra that are not contaminated by emission lines are the Na D lines at 5890, 5896 Å. The low S/N of the absorption lines in our spectra taken near the nucleus of M87 (positions 1, 4, 5, and 6) makes it impossible to determine usefully accurate stellar velocity dispersions from these short exposures. At positions 2 and 3 (radii of 0.″56 and $\approx 2.''1$, respectively), however, we measure dispersions of 490 ± 145 km s^{-1} and 398 ± 66 km s^{-1}, respectively, using the K0 III star F193 as a template and restricting our analysis to a 100 Å region surrounding the Na D doublet. At 0.″56 our measurements exceed previous ground-based measurements of ≈ 400 km s^{-1} (Dressler & Richstone 1990; van der Marel 1994), but are consistent given our large errors. At 2″, the ground-based measurements range from 330 to 395 km s^{-1}, again consistent with our results.

4. THE MASSIVE NUCLEAR ENTITY

The continuum-subtracted Hα + [N II] WFPC2 images discussed by Ford et al. (1994), combined with our FOS spectroscopic measurements, clearly indicate the presence of a rotating disk of ionized gas around the nucleus of M87. The velocity shifts seen in the spectra at positions 5 and 6, located nearly along the major axis, directly show the rotation of the disk and allow us to derive the approximate mass in the inner region of M87 assuming simple circular rotation of the ionized material. Ignoring (for the moment) projection effects from the rotation of positions 5 and 6 off the major axis, the mass interior to radius R is given by $M(R) = (RV^2)/[G \sin^2(i)]$, where V is the measured LOS velocity, G the gravitational constant, and i the inclination of the disk, with $i = 0°$ corresponding to a face-on disk. The higher velocity separation of [O III] compared to the low-ionization lines suggests that the [O III] may be concentrated nearer the nucleus than the lower ionization species. We use $V = 458$ km s^{-1} based on half of the average velocity shift between positions 5 and 6 for the low-ionization species. From narrowband images centered on Hα (Ford et al. 1994), we estimate that the luminosity-weighted centers for positions 5 and 6 for the low-ionization species lie no closer to the nucleus than $\pm 0.''22$, only slightly different from their geometric centers at $\pm 0.''25$. We derive $M(R)$ based on a distance to M87 of 15 Mpc (Jacoby, Ciardullo, & Ford 1990); the geometric centers of the apertures for positions 5 and 6 then project to a distance on the sky of $R = 18$ pc at M87. Our companion *Letter* (Ford et al. 1994) also discusses the imagery which leads us to estimate the inclination angle to be $42° \pm 5°$. With these values, the mass within 18 pc of the nucleus is $M(R < 18 \text{ pc}) \approx 1.9 \times 10^9\ M_\odot$.

The observed blueshifts (with respect to the systemic velocity of M87) at positions 1 and 2, along with the large velocity shifts at positions 5 and 6, suggest that the disk of ionized gas may be in Keplerian rotation about the nucleus of M87. We find that the measured radial velocities for positions 1, 2, 5, and 6 are indeed easily fitted by a model of a relatively thin disk in Keplerian rotation about the nucleus, indicating that the central massive object dominates the integrated stellar mass at these radii. Further evidence of the Keplerian rise in velocity approaching the nucleus is provided by the position 4 (on-nucleus) spectrum, in which the emission lines are broadened to a FWHM ≈ 1700 km s^{-1}.

We have analyzed a simple model in which a thin disk of ionized gas in Keplerian rotation orbits a central mass. Three parameters define the model: the central mass M_C, the inclination i of the disk, and the observed angle θ of the projected major axis of the disk (defined with respect to the line joining the centers of positions 5 and 6). For each of the k observed locations, the predicted radial velocity V_k measured at (projected) radius R_k, and position angle θ_k, is related to the model parameters by

$$V_k^2 = \left(\frac{GM_C}{R_k}\right)\left\{\frac{[\sin^2(i)\cos^3(i)]}{[\cos(\theta+\theta_k)][\cos^2(i)+\tan^2(\theta+\theta_k)]^{3/2}}\right\}.$$

For a grid of these three parameters, we mapped the radial velocity shifts admitted to the FOS aperture at positions 1, 2, 5, and 6. The model reproduces the observed radial velocity data only for a narrow region of the parameter space defined by M_C, i, and θ. Using the result from the images of the disk (Ford et al. 1994) that $i = 42° \pm 5°$, and requiring our model to predict from the spectroscopic data at each point masses consistent to within 20% rms, we determine that (for a distance of 15 Mpc to M87) $M_C = (2.4 \pm 0.7) \times 10^9\ M_\odot$, $i = 42° \pm 5°$, and $1° < \theta < 14°$. This value for θ, derived solely from the spectroscopic measurements, agrees acceptably well with the result $11° < \theta < 20°$ obtained from analysis of the image of the M87 disk. An additional and significant uncertainty in determining the mass of the central object arises from our lack of definitive knowledge of the distance to M87. The value adopted in this *Letter*, D(M87) = 15 Mpc, lies within the range of generally accepted values. Including a distributed stellar component in our models does not significantly affect the mass derived for the central object, because mass distributed similarly to the light from stars (discussed below) cannot reproduce the Keplerian velocity increase near the nucleus.

The nucleus of M87 contains an unresolved, nonthermal continuum source and a centrally peaked distribution of starlight. The central source is unresolved in the FOC ultraviolet imagery by Boksenberg et al. (1992) and the red WF/PC1 imagery by Lauer et al. (1992), both measurements implying that the source is less than 1 pc in radius. Our results agree with spectroscopy by Carter & Jenkins (1992) indicating that the point source emits continuum light which is bluer than that of the stars in the nucleus. We use the surface photometry of Lauer et al. (1992) to estimate the stellar luminosity (excluding the unresolved nonthermal continuum emission source) contained within 0.″25 of the nucleus of M87. They show that an adequate fit to the I-band stellar surface brightness within $R < 3''$ of the nucleus is provided by $\mu(R) \sim R^{-0.26}$, which deprojects in the approximation of spherical symmetry to $\rho_L(R) \sim R^{-1.26}$. Converting to our assumed M87 distance of 15 Mpc, we obtain $\rho_L(R < 9.37 \text{ pc}) \approx 750\ L_\odot \text{ pc}^{-3}$ (I band). Our observations at positions 5 and 6 intersect the (inclined) disk at radius $R \approx 18$ pc. Integrating the luminosity density, we obtain $L_I(R < 18 \text{ pc}) \approx 1.4 \times 10^7\ L_\odot$.

Using the values from the preceding two paragraphs, we obtain $(M/L)_I \approx 170\ (M_\odot/L_\odot)$ within the inner 18 pc of M87 excluding the central unresolved source. Such a large mass-to-

light ratio for stars in M87 seems improbable; furthermore, the required huge number of low-mass stars would not be stable against collisional collapse over the lifetime of a galaxy (cf. Spitzer & Saslaw 1966). Far more likely, we feel, is that the majority of the mass lies within a massive black hole with $M_{BH} = (2.4 \pm 0.7) \times 10^9\ M_\odot$, and that this black hole provides the energy for the nonthermal continuum source contained within $R < 1$ pc emitting $\approx 5 \times 10^7\ L_\odot$ (V band) discussed by Lauer et al. (1992). They also point out that a black hole mass of $3 \times 10^9\ M_\odot$ is compatible with existing ground-based data and the dynamical models of Dressler & Richstone (1990).

With the *HST* now achieving its originally designed angular resolution, we plan further spectroscopic observations of the nuclear region of M87 along the major and minor axes of the gas disk. Spectra within the inner 0".25 region of the nucleus using the FOS 0".09 (square) aperture may reveal yet higher velocity emission lines from gas in Keplerian orbits about the central black hole. The broad emission lines, with wings extending to at least ± 1300 km s^{-1} from V_{sys}, in the spectrum at position 4 (on the nucleus) indicate the presence of very high velocity ionized gas; determining its location should help us better understand the kinematics in the nucleus of M87 and should yield tighter limits on the mass of the central black hole.

We wish to thank the many people within NASA, at the STScI, and at several aerospace companies and universities who produced the FOS, COSTAR, and *HST* to make possible these observations. We especially thank the STS-61 astronauts for their superb job refurbishing the *HST*, carrying out their mission beyond even our most optimistic hopes. Finally, we thank the US taxpayers for funding the FOS science team's research through NASA grant NAG5-1630.

REFERENCES

Boksenberg, A., et al. 1992, A&A, 261, 393
Carter, D., & Jenkins, C. R. 1992, MNRAS, 257, 7p
Dressler, A., & Richstone, D. O. 1990, ApJ, 348, 120
Ford, H. C., & Butcher, H. 1979, ApJS, 41, 147
Ford, H. C., Harms, R. J., Tsvetanov, Z. I., Hartig, G. F., Dressel, L. L., Kriss, G. A., Davidsen, A. F., Bohlin, R., & Margon, B. 1994, ApJ, 435, L27
Jacoby, G. H., Ciardullo, R., & Ford, H. C. 1990, ApJ, 356, 332
Lauer, T. R., et al. 1992, AJ, 103, 703
Sargent, W. L. W., Young, P. J., Boksenberg, A., Shortridge, K., Lynds, C. R., & Hartwick, F. D. A. 1978, ApJ, 221, 731
Spitzer, L., & Saslaw, W. C. 1966, ApJ, 143, 400
van der Marel, R. P. 1994, MNRAS, submitted
Young, P. J., Westphal, J. A., Kristian, J., Wilson, C. P., & Landauer, F. P. 1978, ApJ, 221, 721